AFOSR/AOARD
NBIT Program Phase I (2007-2010)
Part I

Final Report for Year 2
(May 2008 – Apr 2009)

Chapter 1 - Distributed Detection of Attacks/Intrusions and Prevention of Resource-Starvation Attacks in Mobile Ad Hoc Network; Jong Kim (Pohang University of Science of Technology, Korea) and Kang Shin (University of Michigan, USA)

Chapter 2 - Electronic, Photonic and Magnetic Properties of Modified DNAs Complexed with Heavy Metal Ion; Donghoon Choi (Korea University, Korea) and A. J. Steckl (University of Cincinnati, USA)

Chapter 3 – Ultra-Sensitive Biological Detection via Nanoparticle-Based Magnetically Amplified Surface Plasmon Resonance (Mag-SPR) Techniques; Jinwoo Cheon (Yonsei University, Korea) and A. Paul Alivisatos (University of California Berkeley, USA)

Chapter 4 – Hierarchical Carbon Fiber Composites; Kunhong Lee (Pohang University of Science of Technology), Sanggi Lee (Ewha Womans University, Korea) and Thomas Hahn (University of California Los Angeles, USA)

Report Documentation Page

1. REPORT DATE	2. REPORT TYPE	3. DATES COVERED
27 AUG 2009	**FInal**	**01-05-2008 to 01-04-2009**

4. TITLE AND SUBTITLE	5a. CONTRACT NUMBER
Nanoscale and Information Systems with Biological Implications II	**FA48690814047**
	5b. GRANT NUMBER
	5c. PROGRAM ELEMENT NUMBER

6. AUTHOR(S)	5d. PROJECT NUMBER
Pohang Jong Kim; Choi Donghoon; Cheon Jinwoo; Lee Kunhong	5e. TASK NUMBER
	5f. WORK UNIT NUMBER

7. PERFORMING ORGANIZATION NAME(S) AND ADDRESS(ES)	8. PERFORMING ORGANIZATION REPORT NUMBER
Korea Foundation for International Cooperation of Science & ,Technology (KICOS),275-7 Yangjae Dong, Seocho Gu,Seoul Korea (South),KR,275-7	**N/A**

9. SPONSORING/MONITORING AGENCY NAME(S) AND ADDRESS(ES)	10. SPONSOR/MONITOR'S ACRONYM(S)
AOARD, UNIT 45002, APO, AP, 96337-5002	**AOARD**
	11. SPONSOR/MONITOR'S REPORT NUMBER(S)
	AOARD-084047

12. DISTRIBUTION/AVAILABILITY STATEMENT
Approved for public release; distribution unlimited

13. SUPPLEMENTARY NOTES
This document contains results from four different basic research projects under the Phase I of US-Korea NBIT Program (2007-2010). It is the 2nd year results covering research results from 2008-2009.

14. ABSTRACT
Chapter 1 - Distributed Detection of Attacks/Intrusions and Prevention of Resource-Starvation Attacks in Mobile Ad Hoc Network; Chapter 2 - Electronic, Photonic and Magnetic Properties of Modified DNAs Complexed with Heavy Metal Ion; Chapter 3 ? Ultra-Sensitive Biological Detection via Nanoparticle-Based Magnetically Amplified Surface Plasmon Resonance (Mag-SPR) Techniques; Chapter 4 ? Hierarchical Carbon Fiber Composites

15. SUBJECT TERMS

16. SECURITY CLASSIFICATION OF:			17. LIMITATION OF ABSTRACT	18. NUMBER OF PAGES	19a. NAME OF RESPONSIBLE PERSON
a. REPORT **unclassified**	b. ABSTRACT **unclassified**	c. THIS PAGE **unclassified**	**Same as Report (SAR)**	**37**	

Chapter 1

Distributed Detection of Attacks/Intrusions and Prevention of Resource-Starvation Attacks in Mobile Ad Hoc Network

2009-07-10

Korean Principal Investigator (KPI)		US Principal Investigator (USPI)	
Full Name	Jong Kim	Full Name	Kang G. Shin
Affiliation (department)	Pohang University of Science and Technology (CSE)	Affiliation (department)	The University of Michigan (EECS)
Position	Professor	Position	Kevin & Nancy O'Connor Professor
Telephone	+82-54-279-2257	Telephone	+1-734-763-0391
Fax	+82-54-279-2299	Fax	+1-734-763-8094
E-mail	jkim@postech.ac.kr	E-mail	kgshin@eecs.umich.edu

A. Project Goal (of Korean Research Group)

The main purpose of this research is to address the problems of detecting malicious/compromised nodes and preventing resource-starvation attacks in mobile ad hoc networks (MANETs). In this year, we have 2 research items (objectives) like the belows:

- Item 1 : An energy-efficient clustering scheme for IDS

● Item 2 : Low-rate sleep-deprivation attack analysis and detection scheme

In last year, we researched on (A) reliable and efficient detection of malicious nodes, (B) prevention of energy consumption attacks and (C) detection of selfish router in wireless mesh network. Item 1 and 2 are continued from Item (A) and (B), respectively. Item (C) is dropped out because we concluded that it has no practical use.

B. Progress report

1 Item 1 : An energy-efficient clustering scheme for IDS

1.1 Introduction

Cluster-based intrusion detection systems (IDSs) have been proposed in order to improve the performance of mobile ad-hoc networks (MANETs). Conventional cluster-based IDSs have not considered the limitation of the battery power of mobile nodes and the number of clusters to be formed when forming clusters, in which a cluster is composed of a cluster head and cluster members which are located within one-hop from the cluster head. The cluster head monitors the packets of its members to detect the intrusion. The battery power of the cluster head and the number of clusters affect the network lifetime in MANETs. In this research, in order to increase the network lifetime of MANETs, we propose the Distributed Energy Efficient Cluster Formation (DEECF) scheme which exploits the expected residual energy of mobile nodes to select cluster heads and starts the cluster formation from a node which has one neighbor (leaf node) to reduce the number of single-node clusters

1.2 Distributed Energy Efficient Cluster Formation (DEECF) Scheme

In order to increase the network lifetime of MANETs, the DEECF scheme determines the node which has the most expected residual energy as the cluster head and reduces the number of clusters. The expected residual energy is calculated by using the current residual energy and the energy consumption rate, which is the rate that the node consumes energy for transmitting and receiving packets, executing of IDS functionalities and OSs, and so on. In order to reduce the number of clusters, the proposed scheme reduces the number of single-node clusters, which has a cluster head only, because the cluster formations are started from a leaf node.

1.2.1 Cluster formation

The DEECF scheme is composed of two steps, the information exchange step and the cluster formation step. In the information exchange step, each node exchanges its own information, which consists of the node ID, the state, the expected residual energy, and the number of neighbors. Then, in the cluster formation step, each node decides its own role as cluster head or cluster member from the information received from its neighbors in the cluster formation step.

Information exchange step: Nodes exchange the information between neighbors. Initially, every node knows its own information only and is classified as unspecified node.

Each node broadcasts HELLO packets with the information, such as ID and the state, to identify itself to its neighbors. Then, each node calculates its own expected residual energy. After calculating the expected residual energy, each node broadcasts SEND_INFO packet with its own information such as ID, the expected residual energy, and the number of neighbors.

Cluster formation step: This step forms clusters using the information, such as node ID, state, the expected residual energy, and the number of neighbors, received from neighbors of each node. At first, each node compares the degree and ID with unspecified neighbors and decides whether to have a chance to be the cluster head primarily or not. The node with the smallest degree among unspecified neighbors has the chance to be the cluster head. If there is more than one node with the smallest degree, the node with the largest ID has the chance to be the cluster head. The reason is that there may be a network without leaf nodes. In such a case, head selection cannot be performed because there is no deciding rule based on the node ID. The node with the chance to be the cluster head compares the expected residual energy with unspecified neighbors and decides whether to be the cluster head or not. If the node has the most expected residual energy among unspecified neighbors, the node changes the state into CLUSTER_HEAD and broadcasts HEAD_DECLARATION message to neighbors. Otherwise, the node passes the chance to an unspecified neighbor node with the most expected residual energy.

1.2.2 Cluster maintenance

For the energy efficiency of MANETs, we reconstruct clusters periodically according to the cluster reconstruction period in order to form clusters with new cluster heads. However, we should consider a strategy to maintain a cluster when the nodes move to another place during the cluster reconstruction period. To maintain its cluster, each node should know information of its neighbors continuously. Thus, each node needs to transmit periodic HELLO packets, to inform its neighbors of its presence. Basically, each node performs a maintenance algorithm when the information of its neighbors changes. When a node finds out a coming of new neighbor node it decides whether the new node will be included as a new cluster member node or it will make a new cluster itself with the new node. When a node recognizes that one of its neighbors disappears, it decides whether the cluster would be disorganized or the disappearing node would be eliminated from its cluster.

1.3   Simulation

We compared the DEECF scheme with the distributed energy priority cluster formation (DEPCF) scheme [1] and the distributed degree priority cluster formation (DDPCF) scheme [2], in terms of the network lifetime and the number of cluster heads. The DEPCF scheme chooses the node having the most current residual energy as the cluster head. The DDPCF scheme selects the node having the highest degree as the cluster head.
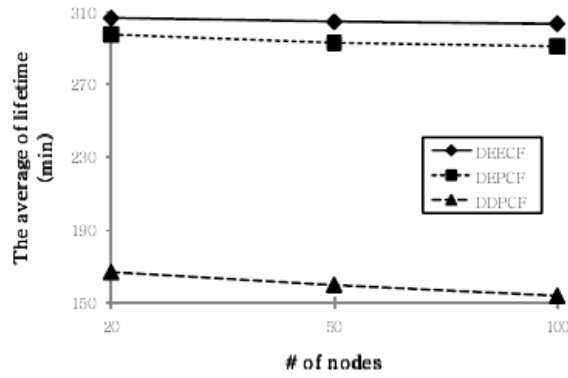
Fig. 1 The average of the network lifetime

Fig. 1 shows the mean of the network lifetime according to the increase of the number of nodes in the network when the initial energy of every node and the energy consumption rate for detection are set to 30 kW and 2.0, respectively. Fig.1 shows that the DEECF scheme has longer network lifetime than the DEPCF and DDPCF schemes by 4 % and 47.5 % in the average case, respectively. This is because the cluster heads in the DDPCF scheme, which are assigned due to the largest degree, are changed only when there is a topology change while the cluster heads in the DEECF scheme and the DEPCF scheme are changed in every cluster reconstruction time due to the change of the residual energy.
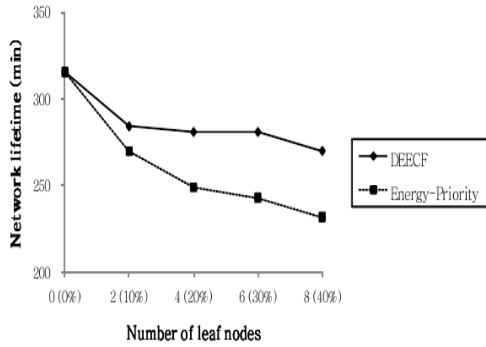
(b) The network lifetime of the DEECF and Energy-Priority scheme
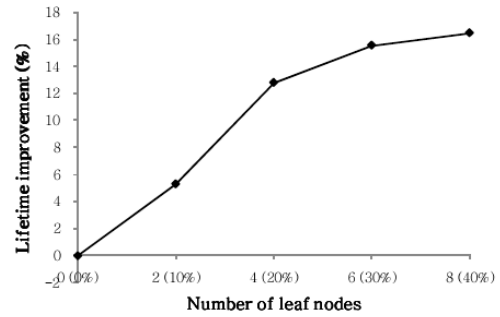
(a) The lifetime improvement of the DEECF scheme over the Energy-Priority scheme

Fig. 2 Comparison of the lifetime with a varying number of leaf nodes (Initial energy = 30kW)

We compare the performance of the DEECF scheme with that of the Energy-Priority scheme in various environments. Fig. 2(a) shows the network lifetime of the DEECF and Energy-Priority schemes according to an increase in the number of leaf nodes in the network. Fig. 2(b) shows the lifetime improvement of the DEECF scheme over the Energy-Priority scheme in the same simulation environment. As the number of leaf nodes increases, the lifetime difference between the DEECF scheme and the Energy-Priority scheme increases linearly with the number of leaf nodes. This is because the start positions of clustering in the Energy-Priority scheme are nodes with the most current residual energy but in the DEECF scheme the start position are leaf nodes. The DEECF scheme reduces the number of single-node clusters because it starts the cluster formation process at the leaf nodes. Thus, as the number of leaf nodes increases, the number of single-node clusters decreases and the network lifetime extends.

2 Item 2 : Low-rate sleep-deprivation attack analysis and detection scheme

2.1 Introduction

MANET has no infrastructure and each node must play special roles like being a router. Thus, availability of each mobile node can be target of security attacks. Especially, as mobile nodes usually have limited battery power, the energy consumption attack such as sleep-deprivation attack is one of main issues in the field of MANET security. With the energy consumption attack, a malicious node can make other nodes tortured with power trouble.

In this research, we propose a novel detection method against sleep-deprivation attack including low-rate sleep-deprivation attack, which is newly defined in this work. Low-rate sleep-deprivation attack is a variant of sleep-deprivation attack which can drain nodes of battery power with low-rate traffic. This attack is hardly detected by previous detection methods such as power-consumption based methods [5,6], because they assume that battery power of node is drained away dramatically. Also if this attack is performed by a multi-hop distant node in the transport/application layer, intermediate nodes on the routing path are difficult to decide whether the relaying packets are malicious or not. Thus, we analyze this low-rate sleep-deprivation attack and propose a novel detection method against sleep-derivation attack.

2.2 Low-rate sleep-deprivation attack

Because mobile nodes are dependent on battery power, it is important to minimize their energy consumption. The energy consumption of the network interface can be significant, especially for small devices. In particular, when operating in ad hoc mode, the idle power consumption is significant, as hosts must maintain their network interfaces in idle mode in order to cooperate in maintaining the ad hoc routing fabric [7].

Power saving techniques, which turn the devices to low-power states when they are not in use, are important techniques to conserve energy for battery-powered wireless devices. The IEEE 802.11 power saving mode is one of the most popular techniques in wireless LAN and multi-hop wireless networks to coordinate the power states of communication devices [3]. Approximately 50% of energy saving can be achieved using the IEEE 802.11 PSM in multi-hop wireless networks [4].

Low-rate sleep-deprivation attack can drain nodes of battery power steady, because they can disturb the mobile device in low-power states with low-rate packets. Usually power saving techniques, such as IEEE 802.11 PSM, is in conjunction with time-out driven policy. Low-rate attack can make mobile devices to keep high-power state by exploiting this characteristic. In our simulation, we can make a mobile node to keep idle state by sending 5 packets per second.

2.3 Detection of sleep-deprivation attack

A most remarkable characteristic of sleep-deprivation attack is *steadiness*. To torture mobile devices consistently, it have to send a certain amount of packets to a target device tirelessly. But this kind of manner gives us a chance to separate malicious packets from

legitimate ones. Usually, legitimate application traffics exhibit multi-faceted burstiness and conglomerate patterns in time-domain. However, under the sleep-deprivation attack, the NIC is mostly under busy state and attack packets are spread uniformly or scattered in time-domain, because it must torture a mobile device continuously. In this work, we measure effects of the *steadiness* in incoming traffic into each node to detection the sleep-deprivation attack.
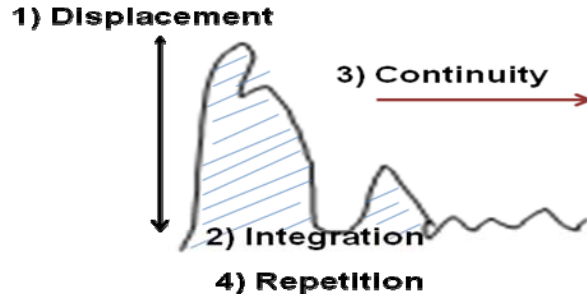

Fig. 3 Features for Maliciousness Decision

To measure the effects of the steadiness, we capture incoming packets toward open ports and count a number of incoming packets per a unit time (0.1sec). This information can be represented as a two dimensional wave pattern like Fig. 3 and the steadiness of the sleep-deprivation attack differentiates its wave pattern from legitimate one. From this wave pattern, we extract four features: displacement, integration of wave, continuity and repetition, which are used to decide whether incoming packets are malicious or not.

To calculate these features in time-domain, we have to maintain packet statistics of each application. But maintenance of packet statistics imposes quite heavy overhead on mobile nodes. To solve this problem, we use a frequency-domain analysis method which can reduce overhead on feature extraction process. Our analysis method is based on discrete cosine transform (DCT), which can be easily implemented; optimally, DCT can be implemented with just 11 multiplications in case of 1-D DCT. To apply our analysis method, we divide incoming wave patterns into a partial wave for each period (0.8 sec). With this analysis method, we can easily extract features of wave patterns without complex calculations.

To decide maliciousness of incoming packets, we calculate an *abnormality score* for each partial wave with extracted features. Using the abnormality score, we can detect sleep-deprivation attacks with the following detection algorithm.

```
If a block is decided as malicious
(1)token1  =  token1 - 1


Upon validation of a normal block to itself
(2) ∆t = the current system clock - time
(3) token1  = min{token1 + ∆t × α, size1}
(4) time  =  the current system clock
(5) if (token1  ≥ 1)
(6)      Ignore
(7) else
(8)      Alert
```

Fig. 4 Detection algorithm

C. Summary

As above mentioned, we have 2 research items. For enhancing the energy efficiency of IDS, we propose an energy-efficient clustering scheme for IDS, called as Distributed Energy Efficient Cluster (DEEC) scheme. Our scheme can reduce the number of monitor nodes and stand-alone nodes. We have conducted extensive experiments to show the energy efficiency of DEEC scheme and to compare it with other clustering schemes.

As a new security attack in MANETs, we introduce a low-rate sleep-deprivation attack, which can exhaust the battery power of mobile devices by sending small amount of packets to them. This attack has not been presented so far as our knowledge and the main targets of this attack are power saving solutions related to networks, such as the 802.11 power saving mode and coordinator-based power saving techniques. In our work, we examine the feasibility of this attack and propose a sleep-deprivation attack detection method including low-rate sleep-deprivation attack detection. We expect our detection method can cope with a low-rate sleep-deprivation attack in the early-stage and wave analysis method can be used to generate quantitative criteria for detecting sleep-deprivation attack.

Reference

1. J. Wu, M. Gao, and I. Stojmenovic, On calculating power-aware connected dominating sets for efficient routing in ad hoc wireless networks. IEEE/KICS Journal of Communications and Networks 4 (2002), 59–70.
2. J. Xin, Z. Yao-Xue, Z. Yue-Zhi, and W. Yaya, A novel ids agent distributing protocol for manets. Lecture Notes in Computer Science 3515 (May 2005), 502–509.
3. R. Zheng, J. Hou and L. Sha, Performance analysis of IEEE 802.11 power saving mode, in: *Proceedings Communication Networks and Distributed Systems Modeling and Simulation Conference (CNDS)* (2004).
4. R. Zheng and R. Kravets. On-demand power management for ad hoc network. In Proceedings of the The 22nd Annual Joint Conference of the IEEE Computer and Communications Societies (INFOCOM), 2003.
5. G. Jacoby, R Marchany and N. Davis, How mobile host batteries can improve network security. IEEE Security and Privacy 2008.
6. T. Buennemeyer, M. Gora, R. Marchany and J. Tront, Battery exhaustion attack detection with small handheld mobile computers, In Proceedings of IEEE International Conference on Portable Information Devices 2007
7. L. Feeney and M. Nilsson, Investigating the energy consumption of a wireless network interface in ad hoc networking environment, IEEE Infocom 2001.

Chapter 2
2nd Year RESEARCH REPORT

♦**Project Title:** Electronic, Photonic and Magnetic Properties of Modified DNAs Complexed with Heavy Metal Ion

♦ **Principal Researcher:** DONG HOON CHOI (KPI, Korea University, Korea)

A. J. Steckl (USPI, University of Cincinnati, USA)

Executive Summary

Program Goal: Understanding of mechanisms for charge transport, optical excitation/emission, magnetism of modified DNA.

Applications: Use modified DNA for electronic, photonic, and magnetic devices: BioLED, BioFET etc.

Uniqueness: Aim to use unique structure of DNA double helix to develop devices with unique and superior characteristics.

Approaches: Collaboration between basic chemistry (KU) and device engineering (UC). KU is introducing intelligent functionality in DNA materials *via* synthetic approaches and UC is developing DNA thin films and novel device architectures based on the DNA materials.

Status and progress: at Korea Univ., new organic soluble DNAs were synthesized using various lipid units. CTMA-DNA, Cz-DNA, and Cc-DNA were employed to study their photophysical, photochemical, and electronic properties. Mn-doped DNA was also used for studying the magnetism. At UC - Study of DNA thin films complexed with luminescent metal-organic compound (SRh) has yielded evidence of intercalation. UC collaboration also with AFRL-Materials Directorate (J. Grote, R. Naik) on materials properties.

Research during next period: At Korea University, phosphorescence and electrophosphorescence were studied using the Cz-DMA host after doping a soluble iridium complex we developed. Cc-DNA will be utilized as a dielectric layer for organic thin film transistor. Nanofiber will be prepared through electro-spinning technique with and without metal nanoparticles. In the field of magnetism, we will dope iridium complex or stable radicals to prepare the samples. At UC, bio-light-emitting diodes (BioLEDs) incorporating DNA doped with SRh will be fabricated and characterized. Under our collaboration, the first co-work will be presented about photophysical properties of guest-host system or covalently bonded system.

1. INTRODUCTION

Among the rich world of naturally occurring biomaterials probably none is more important and more fundamental than DNA (deoxyribonucleic acid), the polymeric molecule that carries the genetic code in each living organism. It is not, therefore, not surprising that the nascent field of DNA photonics which combines *light* with the molecule of *life* excites the interest of the wider scientific community. Based on interaction of DNA with light, and with other segments of the electromagnetic spectrum, we can deduce the influence of electric and magnetic fields on the molecular unit in the DNA structure. Therefore, DNA is an ideal candidate for us to study electronic, photonic, and magnetic effects on biopolymers and to investigate related devices.

Organic and polymer chemists are able to introduce many intelligent functions in a material *via* various synthetic approaches. Electrical engineers are eager to exploit unusual material properties in designing novel or improved devices. However, an optimum strategy is to combine the skills and interests of chemists and electrical engineers in order to take full advantage of the many hidden "talents" of DNA. By working together, the KU-UC team aims to reach the point where one can "tune" DNA such that it can display the desired specific properties for application to electronics, photonics, magnetism, biotechnology or other fields that have not been envisioned yet. That will indeed be a great accomplishment both in science and in technology.

2. VISION

This proposal aims to build an international collaboration between groups at Korea University (KU) and at the University of Cincinnati (UC) that are at the forefront of research on the properties of solid state DNA and application of these unique properties to novel devices.

3. GOALS/OBJECTIVES

- In-depth examination of the properties of solid state and modified DNAs.
- Application of modified DNA to electronic, photonic, and magnetic applications.
- Understanding of mechanisms for charge transport, optical excitation/emission and magnetism of modified DNA.

4. Researchers

♦ **Principal Investigator(Korea): Dong Hoon Choi, Associate Professor**
Department of Chemistry, KOREA UNIVERSITY, 5-1 Anam-dong, Sungbuk-gu, Seoul 136-701 KOREA

Professor: 2, Post Dr.: 1, Master Course Student: 1

♦ **Principal Investigator(US): Andrew Steckl, Gieringer Professor, Ohio Eminent Scholar**
Department of Electrical Engineering, UNIVERSITY OF CINCINNATI, 899 Rhodes Hall, Cincinnati Ohio 45221-0030 USA

Professor: 2, Post Dr.: 1, PhD student: 2

1.5 RESEARCH PROGRESS

A. Korea University

1.5.1. Photoluminescence Behaviors of Organic Soluble DNA bearing Carbazole and Pyrene Derivatives as Side-Chain Substituents; Effect of the Copolymer Structure on the Förster Energy Transfer Process (Journal of Polymer Sci. Part A, in press (2009))
► Organic soluble DNA bearing two different fluorophores in the side chain was prepared by reacting purified DNA with the cationic molecules 9-(12-bromododecyl)-

9H-carbazole and (E)-1-(4-(12-bromododecyloxy)styryl)pyrene in water. Two homopolymers (CzDNA and PyDNA) and random copolymers (CzDNA-co-PyDNA) were prepared successfully. (See Figure 1)
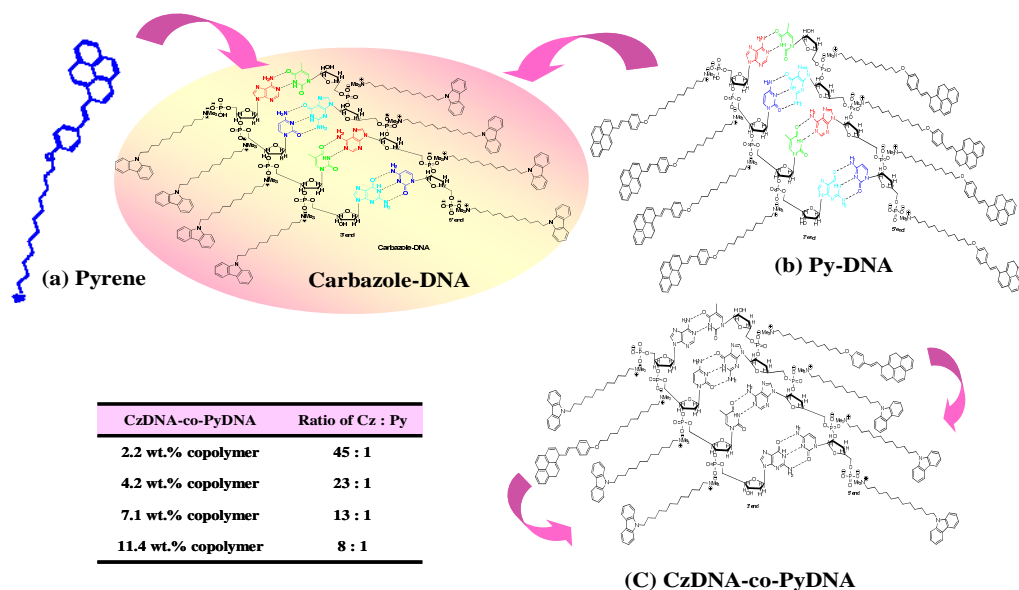

CzDNA-co-PyDNA	Ratio of Cz : Py
2.2 wt.% copolymer	45 : 1
4.2 wt.% copolymer	23 : 1
7.1 wt.% copolymer	13 : 1
11.4 wt.% copolymer	8 : 1

Figure 1. Cz-DNA and pyrene based Fluorescent Polymer Systems. (a) Guest-host system, (b) Polymer blend, (c) Copolymer system.
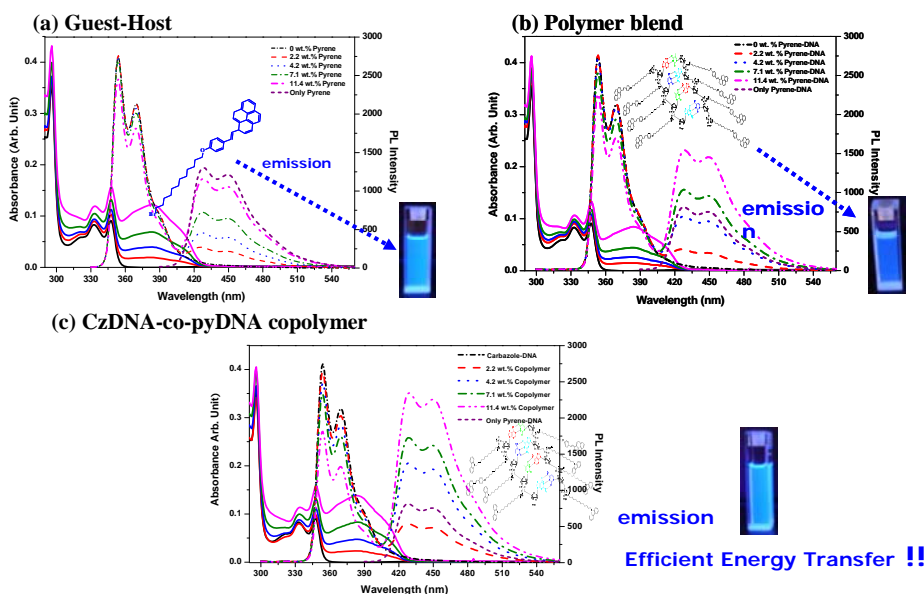

Figure 2. Absorption and PL spectra of three polymeric samples in solution states with pyrene moiety concentrations. A: guest-host systems, guest is (E)-1-(4-(12-bromododecyloxy)styryl)pyrene, 5 and host is CzDNA; B: blends of CzDNA and PyDNA, C: CzDNA-co-PyDNA copolymers. *Concentrations of pyrene moiety: (a) 0 wt%, (b) 2.2 wt%, (c) 4.2 wt%, (d) 7.1 wt%, and (d) 11.4 wt%. *Solid lines: absorption spectra; Dashed lines: PL spectra.

In Fig. 2, the absorption and PL spectra in solution states are illustrated with the

concentrations of pyrene moieties. When the guest-host system solution was irradiated at 290 nm, we could observe the emission behavior of the pyrene moiety at 400–500 nm. However, when 5 reached 7.1 wt%, no decrease in carbazole emissions at 354 and 370 nm was observed. At 11.4 wt% pyrene moiety, a small decrease in emission intensity at 354 (370) nm was observed. Therefore, this indicates that at concentrations lower than 11.4 wt% for the pyrene unit, no energy transfer occurs; emission is only attributed to the direct excitation of the pyrene unit at 290 nm. (Fig. 2a). In Figs. 2b and 2c, we can observe different emission spectral behavior of the guest-host system. When we blend two homopolymers with the concentration of PyDNA, at 7.1 wt% the emission intensity at 354 (370) nm starts to decrease; this implies that two different DNA polymer chains are assembled together to reduce the distance between the carbazole and pyrene moieties. A clear difference can be observed in the copolymer system. As can be seen in Fig. 2c, even when the pyrene unit is at 2.2 wt% in the polymer, the energy transfer from carbazole to pyrene is clearly observed and enhances the emission intensity at 428 (449) nm due to a more efficient energy transfer process.
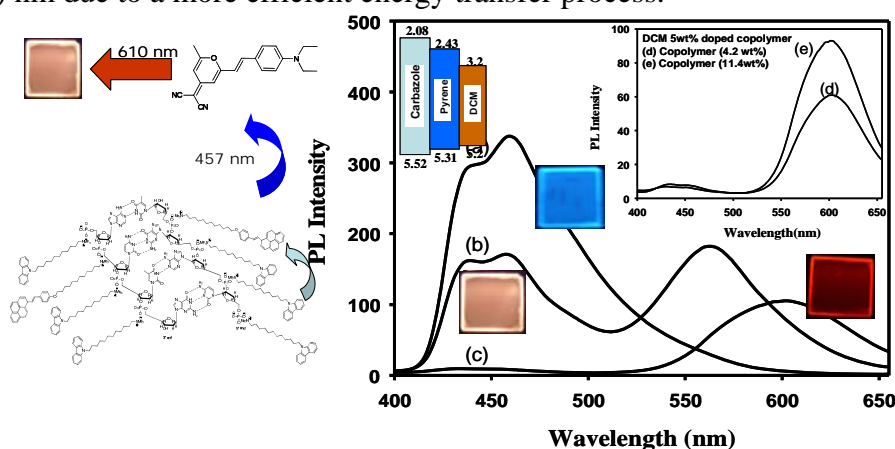

Figure 3. PL spectra of the copolymer film bearing 11.4 wt% pyrene moieties and its mixtures with DCM dye concentrations. (a) Copolymer (11.4 wt%), (b) Copolymer (11.4 wt%) doped with 0.3 wt% DCM, and (c) Copolymer (11.4 wt%) doped with 5.0 wt% DCM. *Inset: (d) Copolymer (4.2 wt%) doped with 5.0 wt% DCM and (e) Copolymer (11.4 wt%) doped with 5 wt% DCM. *Sample: film (thickness ~60 nm).

► Cascade energy transfer from carbazole moieties to DCM dye

To examine the cascade energy transfer process using the DNA-based copolymers, DCM was mixed into CzDNA-co-PyDNA (11.4 wt% pyrene moiety). We fabricated thin films on a quartz substrate to measure PL spectra with excitation at 335 nm. As seen in Figure 3, the emission intensity of heavily pyren-loaded copolymer is the smallest of the samples. PL studies of the doped matrix demonstrated that a significantly high energy transfer from excited pyrene moiety in the copolymer to DCM was achieved. We added 0.3 wt% of DCM into the copolymer. In Fig. 3, the spectrum in (b) shows two emission bands together, which implies partial energy transfer from excited pyrene to DCM in the ground state. When adding 5.0 wt% DCM dye into the copolymer, the emission of pyrene unit was almost quenched and red emissions were clearly observed. Another interesting feature is in the inset of Fig. 3. Under identical concentrations of doping DCM dye, two copolymer films showed different emission intensities. The emission intensity of curve (e) is slightly larger than that of curve (d). The DCM emission is larger, indicating that the introduction of higher concentrations of

DCM dye can loosen the aggregation of the pyrene moieties.

1.5.2. Electrophosphorescence of Cz-DNA bearing Ir(Cz-ppy)₃

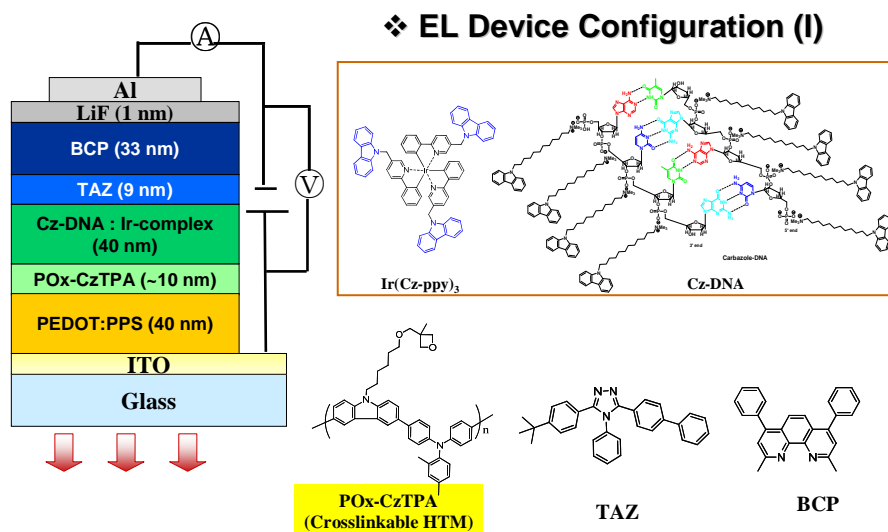Figure 4. Molecular structures of Ir(Cz-ppy)₃, Ir(ppy-Cz)₃, POx-CzTPA, Cz-DNA, TAZ, and BCP. The device configuration of electrophosphorescent PLED.

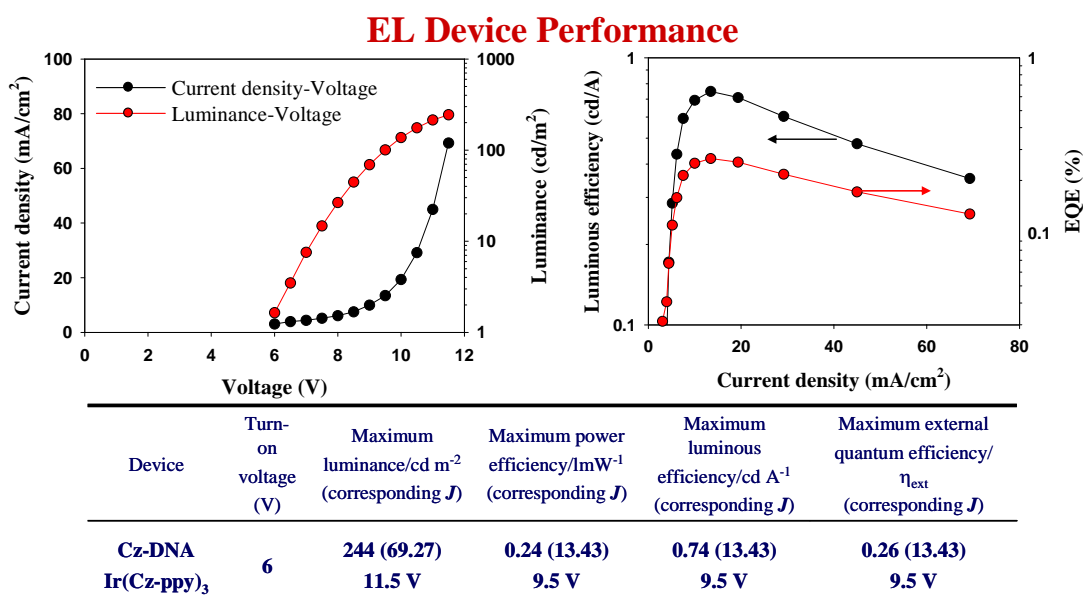| Device	Turn-on voltage (V)	Maximum luminance/cd m⁻² (corresponding *J*)	Maximum power efficiency/lmW⁻¹ (corresponding *J*)	Maximum luminous efficiency/cd A⁻¹ (corresponding *J*)	Maximum external quantum efficiency/ η_ext (corresponding *J*)
Cz-DNA Ir(Cz-ppy)₃	6	244 (69.27) 11.5 V	0.24 (13.43) 9.5 V	0.74 (13.43) 9.5 V	0.26 (13.43) 9.5 V

Figure 5. (Left) Dependence of current density and luminance on the applied voltage. (Right) Dependence of luminous efficiency and external quantum efficiency on the current density. Measured data for device performances

 The maximum brightness of the Cz-DNA based PLED was around 244 cd/m^2 (at 69.27 mA/cm^2). Figure 5 displays the dependence of the luminous efficiency and external quantum efficiency on the current density for the electrophosphorescent device. The maximum luminous efficiencies of the device were determined as 0.74 cd/A (at 13.43 mA/cm^2, η_{EQE} = 0.26% at 13.43 mA/cm^2). The devices will be modified after adding the

electron blocking layer and some more auxiliary layers to improve the performances.

References

[1] Watson JD, Crick FC. Nature 1953;171:737-8.

[2] Steckl AJ. Nat Photonics 2007;1:3-5.

[3] Stadler P, Oppelt K, Singh TB, Grote JG, Schwoediauer R, Bauer S, Piglmayer-Brezina S, Baeuerle H, Sariciftci D, Serdar N. Org Electron 2007;8:648-54.

[4] Agen JA, Li W, Steckl AJ, Grote JG. Appl Phys Lett 2006;88:171109.

[5] Condon A. Nature reviews 2006;7:565-75.

[6] Erkkila KE, Odom DT, Barton JK. Chem Rev 1999;99:2777-95.

[7] Armitage BA. Top Curr Chem 2005;253:55-76.

[8] Lipscomb LA, Zhou FX, Presnell SR, Woo RJ, Peek ME, Plaskon RR, Williams LD. Biochemistry 1996;35:2818-23.

[9] Ihmels H, Otto D. Top Curr Chem 2005;258:161-204.

[10] Wood KC, Azarin SM, Arap W, Pasqualini R, Langer R, Hammond PT. Bioconjugate Chem 2008;19:403-5.

B. University of Cincinnati

The unique structure of DNA has provided opportunities for novel and improved devices: photonics [1] , electronics [2], spintronics [3], etc. We have previously reported [4, 5] the beneficial use of DNA nanometer thin films in OLEDs. Stimulated emission from lasing structures containing DNA gain medium doped with organometallic dye molecule sulphorhodamine (SRh) has shown quite a low threshold [6]. The SRh molecule is shown in Fig. 1. In the report period we have investigated the central issue of whether SRh is actually intercalated in the DNA structure and, conversely, whether the DNA structure, heavily loaded with SRh, preserves its chirality. Chirality of molecules is investigated by performing circular dichroism (CD) spectroscopy [7]. The sample to be considered is represented in the center of the CD spectrometer. Since the DNA molecule exhibits chirality, it is clear that a CD spectrum will be present in the absorption region of DNA. Far less obvious is that a CD spectrum will be observed in the absorption region of the non-chiral SRh molecule, once combined with DNA.
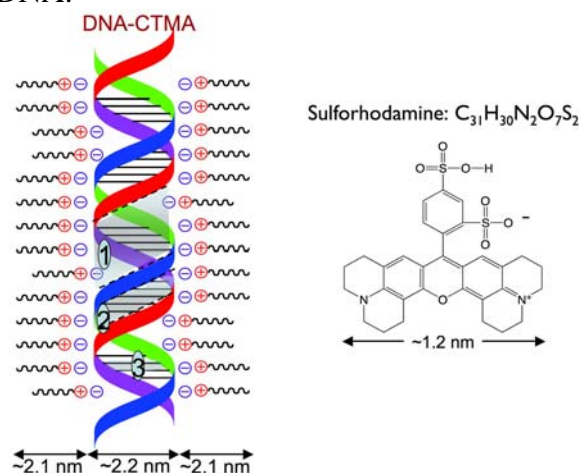

Fig. 1 The DNA-CTMA double helix polymer and the sulforhodamine molecule. The

DNA double helix indicates possible locations for the binding of the SRh molecule: (1) major groove; (2) minor groove; (3) intercalation between base pairs.

Results and Discussion

CD signal is plotted against wavelength for four samples in Fig. 2. Considered here are samples containing DNA:CTMA only and those containing DNA:CTMA with 5 wt.% SRh. In this case, the CD signal is shown in the DNA absorption region. Results for both thin film and solution samples are included. Here, there is no obvious correlation between the presence of SRh and the strength of the DNA CD signal. The strength of the signals for the thin film samples are stronger than those of the solution samples. This is typical of our samples due to the concentrated nature of the thin films, putting more material in the path of the CD spectrometer.

In Fig. 3, a similar plot is provided, but for the SRh absorption wavelength region. Displayed here are spectra for samples containing 2.5% and 15% SRh to DNA:CTMA by weight. Both thin film and solution spectra are provided. It is, again, observed that the thin films result in a CD spectrum of greater intensity than the solution samples. Notable, is the increase in amplitude with an increase in SRh concentration, for both thin film and solution cases.

A summary of the peak-to-peak CD amplitude (in the DNA absorption region) of the samples investigated is shown in Fig. 4. There is no obvious correlation in solution samples, between SRh concentration and DNA CD intensity. For thin films, the CD signal demonstrates a slight increase in intensity, in combination with SRh, with the exception of a decrease in signal at the highest concentration (25%) of SRh. It is possible that enough SRh molecules are finally attached to the DNA molecule, in the this case, to begin disturbing the chirality of the spiral.

Fig. 3 also shows peak-to-peak CD amplitude in the SRh absorption region. Here, there is a clear increase in CD signal strength, with increasing SRh concentration. This observation demonstrates that SRh takes on the chiral nature of the DNA molecules with which it has been combined. The plot flattens at higher concentrations of SRh, indicating a saturation effect, wherein the sample contains more SRh than can readily bind to the DNA.

Summary of Current Results

We have considered the important question of the physical nature of the association between DNA and SRh. In doing so, we have used CD spectroscopy to demonstrate that SRh takes on the chiral nature of DNA in a mixture and, thus, is intercalated in the DNA. Also, it has been shown that this intercalation enhances the natural chirality of the DNA molecule, below a SRh concentration of 25% in thin films.
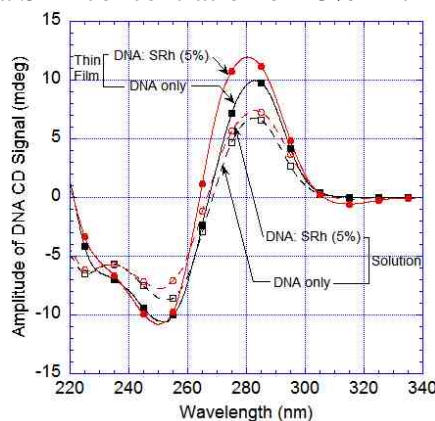

Fig. 2 CD signal (mdeg) for SRh absorption region vs wavelength (nm). DNA only

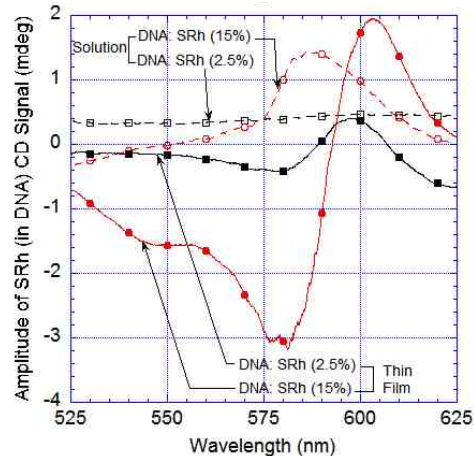and DNA:SRh 5% are included in both solution and thin film forms.

Fig. 3   CD signal (mdeg) for DNA absorption region vs wavelength (nm).   DNA only and DNA:SRh 5% are included in both solution and thin film forms.
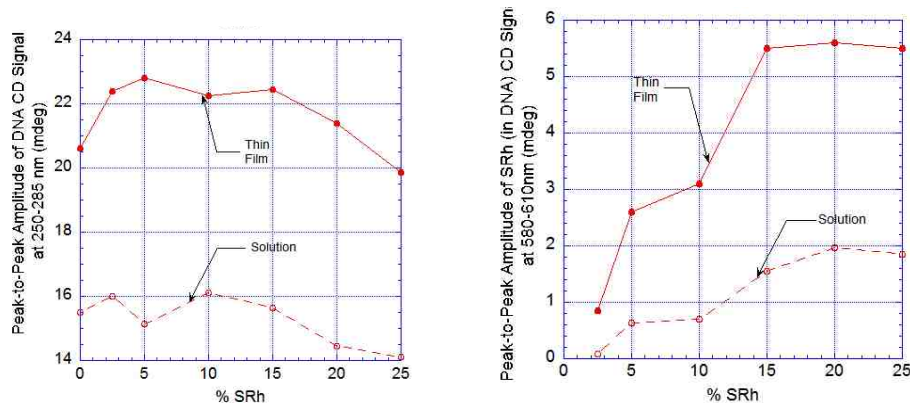

Fig. 4   Peak-to-peak CD Signal (mdeg) for SRh and DNA regions versus SRh concentration (%).

[1]   A. J. Steckl, "DNA - a new material for photonics?," *Nature Photonics,* vol. 1, p. 3, January 2007 2007.
[2]   B. Singh, N. S. Sariciftci, J. Grote, and F. K. Hopkins, "Bio-organic-semiconductor-field-effect-transistor based on deoxyribonucleic acid gate dielectric," *Journal of Applied Physics,* vol. 100, p. 024514, 2006.
[3]   C. H. Lee, E.-D. Do, Y.-W. Kwon, D.-H. Choi, J.-I. Jin, D.-K. Oh, H. Nishide, and T. Kurata, "Magnetic Properties of Natural and Modified DNAs," *Nonlinear Optics, Quantum Optics,* vol. 35, pp. 165-174, 2006.
[4]   J. A. Hagen, W. Li, A. J. Steckl, and J. G. Grote, "Enhanced emission efficiency in organic light-emitting diodes using deoxyribonucleic acid complex as an electron blocking layer," *Applied Physics Letters,* vol. 88, p. 171109, 2006.
[5]   J. A. Hagen, W. X. Li, H. Spaeth, J. G. Grote, and A. J. Steckl, "Molecular Beam Deposition of DNA Nanometer Films," *Nano Lett.,* vol. 7, pp. 133-137, 2007.
[6]   Z. Yu, W. Li, J. A. Hagen, Y. Zhou, D. Klotzkin, J. G. Grote, and A. J. Steckl, "Photoluminescence and lasing from DNA thin films doped with sulforhodamine," *Applied Optics,* vol. 46, p. 7, 20 March 2007 2007.
[7]   A. Rodger and B. Norden, *Circular Dichroism & Linear Dichroism.* Oxford: Oxford University Press, 1997.

1.6 Summary

This research is based on collaboration between Korea University (KU) and the University of Cincinnati (UC). The topic of the research is the investigation of the electronic, photonic and magnetic properties of DNA and the use of the unique properties of DNA in developing novel and improved devices. Researchers of Korea University are introducing many intelligent functions in a natural DNA *via* various synthetic approaches. UC are trying to exploit unusual material properties in designing novel or improved devices.

Now, DNA-surfactant complexes themselves and DNA-surfactant complexes doped with fluorescent or phosphorescent dyes were prepared by Korean Researchers, but characterization of chemical and physical properties are now under way. And also UC tried to make a various devices with MBD technique and are obtaining the current-voltage (I-V), current-light (I-L), and light-time (L-t) characteristics and so on. In the workshop held in Seoul, the researcher from UC took some modified DNA samples to his laboratory. They will use them for fabricating BIOLED and some electronic devices to measure the electrical properties. In particular, the Korean PI's group recently succeeded to spin the nanofiber using organic soluble DNAs *via* elecrospinning technique. The diameter was optimized to be around 60-100 nm. Metal nanoparticles can be doped into the fiber with the concentration. The characterization of the electrical properties is now in progress.

Chapter 3

The Final Report

Title: Ultra-Sensitive Biological Detection via Nanoparticle-Based Magnetically Amplified Surface Plasmon Resonance (Mag-SPR) Techniques

Principal Investigator:

Profs. Jinwoo Cheon (Yonsei University.)

Telephone: +82-2-2123-5631

E-mail: kenneth. jcheon@yonsei.ac.kr

Contract Number: FA2386-01-4060

AOARD Reference Number: AOARD-094060

AOARD Program Manager: John Seo

Period of Performance: 2 year

Submission Date: 10 Jul. 2009

Ultra-Sensitive Biological Detection via Nanoparticle-Based Magnetically Amplified Surface Plasmon Resonance (Mag-SPR) Techniques

(자성 증폭 나노 입자를 이용한 초고감도 SPR 생체 진단기술 개발)

P.I.s: Profs. Jinwoo Cheon (Yonsei U.) & A. Paul Alivisatos (U. of California, Berkeley)

Research Goal: The ultimate goal of this project is the development of ultra-sensitive, and high-performance Mag-SPR (Magnetically Amplified Surface Plasmon Resonance) nano-bio sensing technique by using integrated nanoparticles.

Research Purpose of Phase II: Development of Mag-SPR probes and detection of Mag-SPR probes in live cell at the single molecule level
- Development of multi-core Mag-SPR probes
- In-situ imaging of multi-core Mag-SPR probes in live cells
- Development of proto-type magnetic tweezers

Research Contents

1. Fabrication of multi-core Mag-SPR probes (Korea):

- During the phase II research period, we have tried to synthesize new-type Mag-SPR probes which contain multi-core magnetic nanoparticles in order to increase the magnetic properties of Mag-SPR probes.

- We selected <u>ZnMn</u>-doped <u>M</u>agnetism-<u>E</u>ngineered <u>I</u>ron <u>O</u>xide (ZnMn-MEIO, $(Zn_{0.4}Mn_{0.6})Fe_2O_4$) nanoparticles with high magnetism and crystalinity as the magnetic core and synthesized by a high temperature nonhydrolytic organometallic precursor decomposition route (<u>Lee & Cheon *et al, Nat. Med.* **2007**, *13*, 95 and Jang & Cheon *et al, Angew. Chem. In. Ed.* **2009**, *48*, 1234</u>). Obtained ZnMn-MEIO nanoparticles possess 15 nm size with high monodispersity ($\sigma \approx 5$ %) (Figure 1a and 1b) and enhanced magnetic properties (175 emu/g (Zn+Mn+Fe)) (Figure 1c).
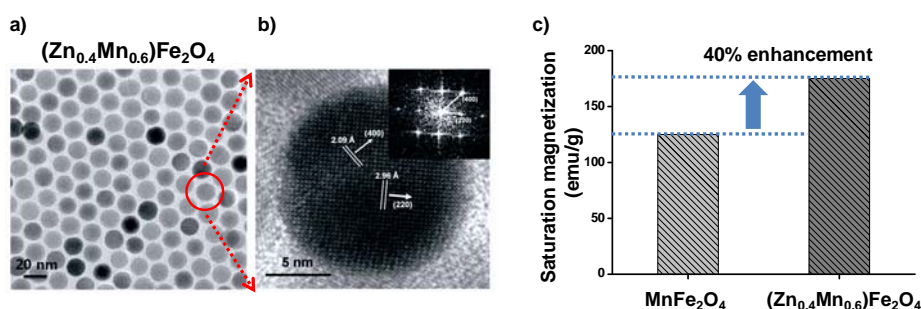
Figure 1. Transmission electron microscope (TEM) image and saturation magnetization value of ZnMn-MEIO (a) TEM image, (b) HR-TEM image of 15nm ZnMn-MEIO, (c) magnetic properties of ZnMn-MEIO compared to Mn-MEIO.

- Then, these ZnMn-MEIO nanoparticles were coated with dielectric SiO_2 via Stober method and subsequently coated with gold shells with high plasmonic properties and excellent bio-compatibility. Figures 2b and 2c show transmission electron microscopic images of multi-core ZnMn-MEIO@SiO_2 and ZnMn-MEIO@SiO_2@Au nanoparticles, respectively. Obtained multi-core ZnMn-MEIO@SiO_2@Au nanoparticles are ~ 80 nm in size with high monodispersity where the thickness of SiO_2 and Au shells are ~ 20 nm and ~ 10 nm, respectively. Our multi-core ZnMn-MEIO@SiO_2@Au nanoparticles show strong plasmonic peak around 600 nm.
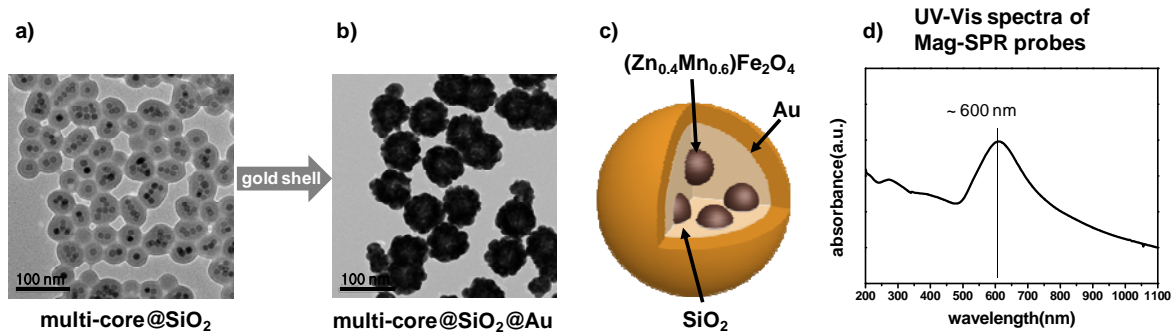

Figure 2. Transmission electron microscope image of (a) ZnMn-MEIO@SiO2, (b) ZnMn-MEIO@SiO_2@Au, and (c) ZnMn-MEIO@SiO_2@Au nanoparticles and (d) UV/Vis absorption spectra of ZnMn-MEIO@SiO_2@Au nanoparticles.

2. In-situ imaging of single multi-core Mag-SPR probes in live cells

- In order to use our Mag-SPR techniques for single molecule imaging in live cells, we chose Her2/neu cancer markers expressed on the membrane of SK-BR-3 breast cancer cells as a case study. We first conjugated Mag-SPR nanoparticles with protein A-Herceptin complexes by using the interaction between Au shell and thiolated protein A-Herceptin complexes. Then, we treated SK-BR-3 cells with nanoparticle-Herceptin conjugates. Since Herceptin is a known antibody that specifically binds to the Her2/neu receptor, our nanoparticle-Herceptin conjugates can specifically label Her2/neu receptors that are distributed on the membrane of SK-BR-3 cells. After addition of the nanoparticle-Herceptin conjugates, we monitored the antibody (*i.e.* Herceptin)-antigen (*i.e.* Her2/neu) interaction *in situ* by using a dark field microscope with a color CCD.
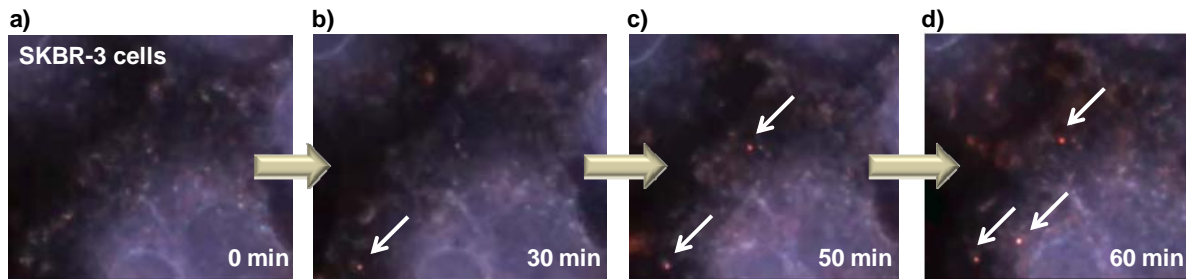
Figure 3. Real time imaging of antigen-antibody interaction in live cells by using Mag-SPR dark-field microscopy (a) 0 min, (b) 30 min, (c) 50 min, and (d) 60min

- We have successfully imaged single multi-core Mag-SPR nanoprobes through our dark-field microscopy (Figure 3a-d). This means that Mag-SPR-Herceptin conjugates recognize HER2/neu receptors expressed on SK-BR-3 cell lines.

3. Development of proto-type magnetic tweezers

- To have the ability to precisely manipulate biomolecule movement, it is necessary to develop a magnetic tweezer which can localize magnetic field to the region-of-interest. For this purpose, we setup a proto-type magnetic tweezer system, described in Figure 4. This is composed of 3-dimensional stage controller and a permanent magnet and superparamagnetic micro tip with of end-tip size of 5 um.
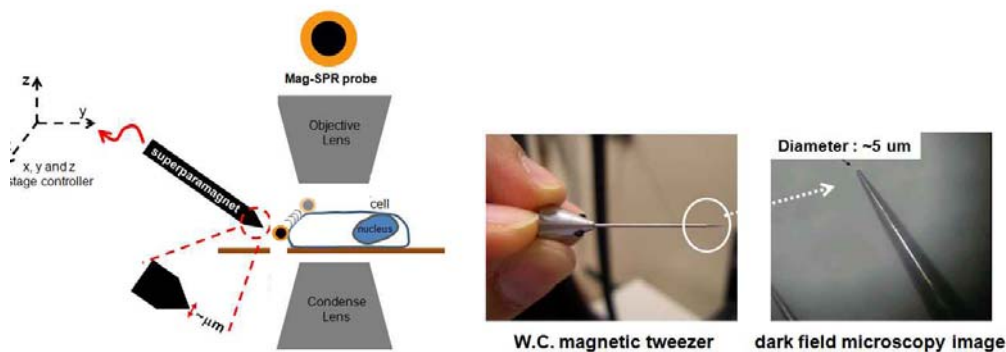

Figure 4. Proto-type magnetic tweezer system

Conclusion

- We have successfully fabricated multi-core Mag-SPR probes
- We have observed successfully in-situ imaging of single multi-core Mag-SPR probe in live cells
- We have successfully installed proto-type magnetic tweezer system.

Hierarchical Carbon Fiber Composites

KPI : Kun-Hong Lee, Ph.D. (POSTECH)

Co-KPI : Sang-gi Lee, Ph.D. (Ehwa Women's University)

USPI : H. Thomas Hahn, Ph.D. (UCLA)

2nd year Report

Research Title: Hierarchical Carbon Fiber Composites Task I: Formation of nanostructures on the surfaces of carbon fibers

Research Institute: Department of Chemical Engineering, POSTECH

Principal Investigator: Professor Kun-Hong Lee

Co-Investigator: Eugene Oh

1.1. Objective

To form various nano-structures on the surface of carbon fibers (CFs) to develop hierarchical carbon fiber composites.

1.2. Accomplishments

Two different nano-structures were successfully synthesized on the surface of carbon fibers. The first one is Silicon carbide (SiC) nanowires. They were synthesized by the carbonthermal reduction of tungsten oxide and graphite. Fig. 1(a) shows the details of the synthesis process in a schematic fashion, while Fig. 1(b) shows the SEM images of synthesized SiC nanowires.
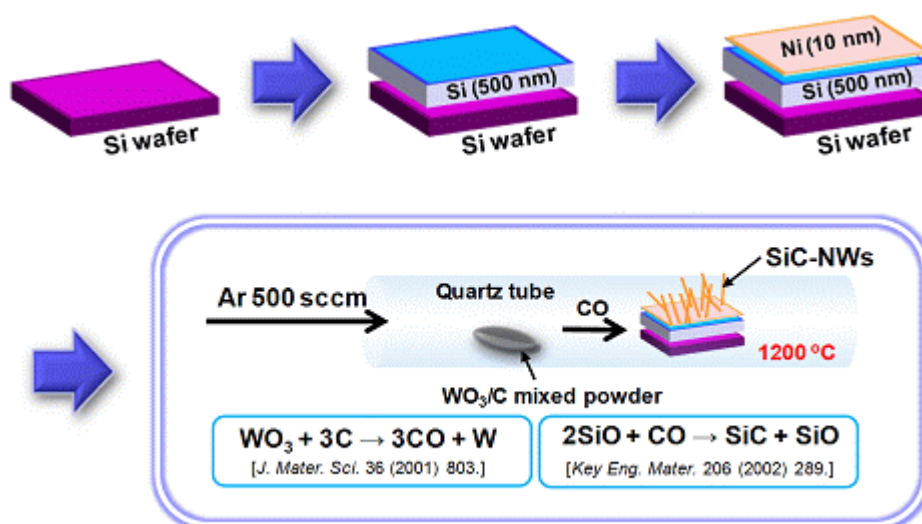

$$WO_3 + 3C \rightarrow 3CO + W$$
[J. Mater. Sci. 36 (2001) 803.]

$$2SiO + CO \rightarrow SiC + SiO$$
[Key Eng. Mater. 206 (2002) 289.]

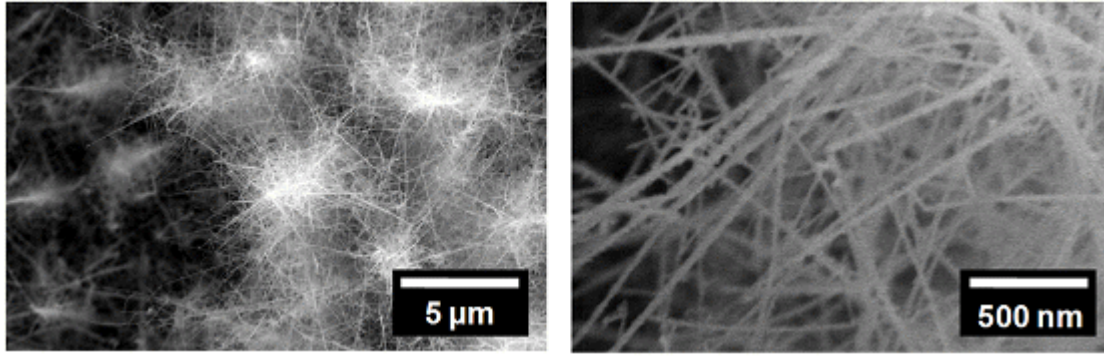**Fig. 1. (a) Schematic diagram of the carbothermal synthesis process**

Fig. 1. (b) SEM photograph of synthesized SiC nanowires

The second nanomaterial synthesized on the surface of carbon fibers is zinc oxide (ZnO) nanowires. ZnO nanowires were synthesized by the hydrothermal reaction of zinc nitrate and hexametylenetetramine. Fig. 2 schematically shows the sample prepared before hydrothermal synthesis. The thin layer of Zn was convered to ZnO nanowires during hydrothermal synthesis. The SEM image clearly shows the hexagonal nanowires on the surface of carbon fibers, while XRD data proves that they are true ZnO.
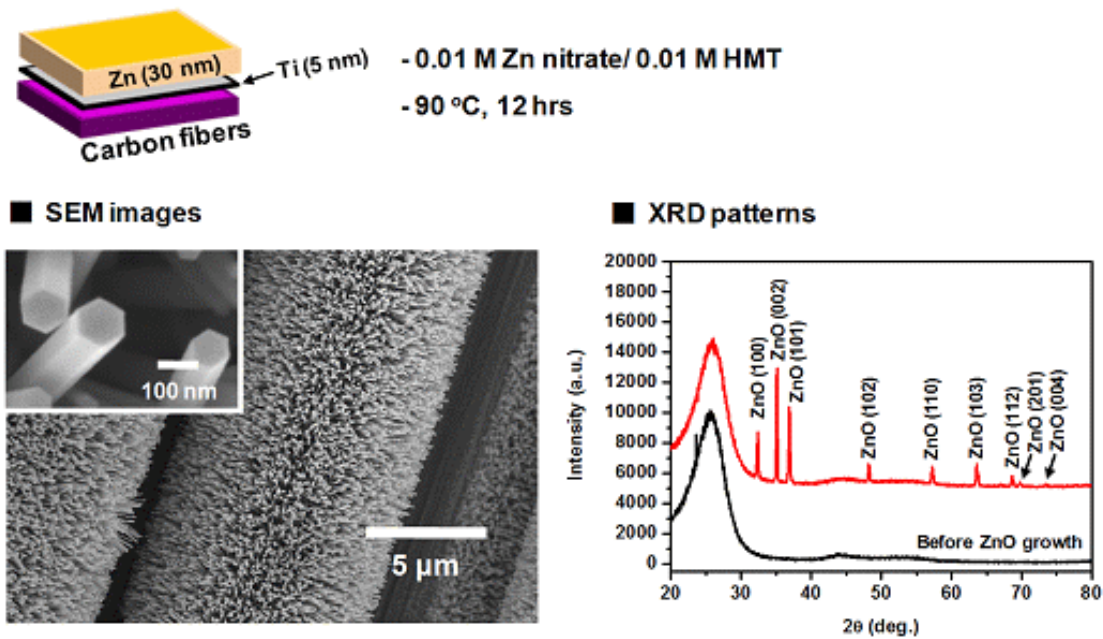

Fig. 2. SEM images and XRD analysis of the carbon fibers covered with ZnO

3

nanowire arrays along the radial direction.

We were able to control the diameter of ZnO nanowires. Different concentration of the starting solution resulted in the ZnO nanowires of different diameters as shown in the SEM images of Fig. 3.
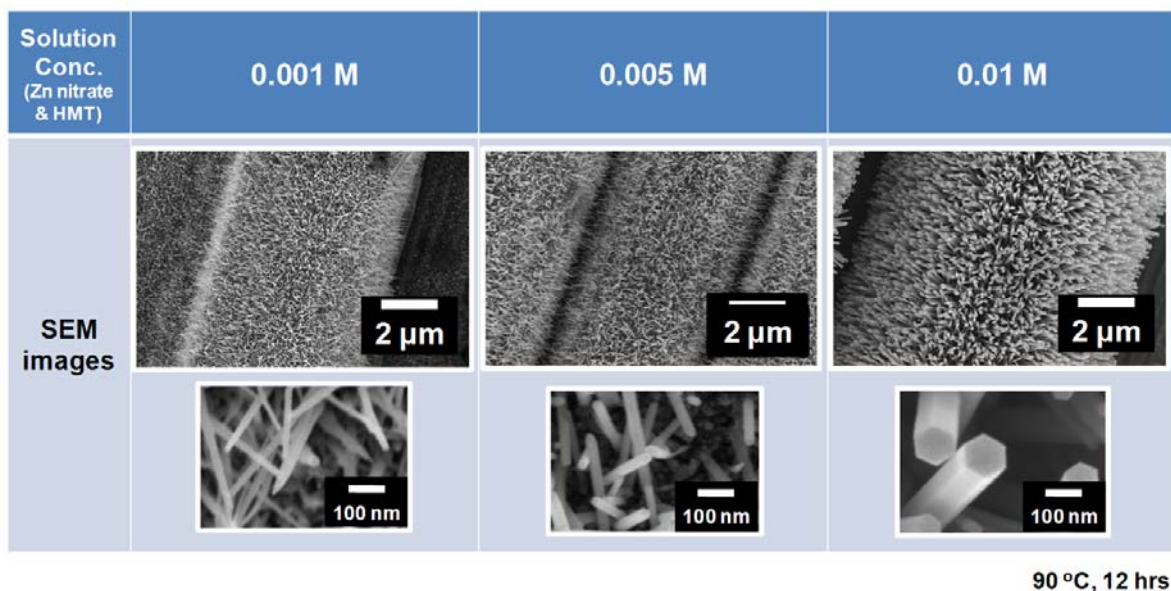

Fig. 3. SEM images of ZnO nanowire arrays with different diameters on the carbon fibers.

Research Title: Hierarchical Carbon Fiber Composites Task II: Ionic liquid-carbon nanotube hybrid materials

Research Institute: Department of Chemistry and Nano Science, Ewha Womans University

Principal Investigator: Professor Sang-gi Lee

Co-Investigator: Dr. Yu Sung Chun, Ju Yeon Shin and Cho-Long Park

2.1. Objective

The aim of the research project is preparation of covalently functionalization of carbon nanotubes with ionic liquid moiety having having polymerizable nobonene, epoxy, and amine functional groups, which can be utilized for the development of hierarchical carbon fiber composites in Task III.

2.2. Status of Effort

In first year, we have developed a functionalization method for CNTs with ionic liquid having epoxy group. To improve the mechanical properties of the epoxy resin composites in Task III, a IL-CNTs having amine group is required. To accomplish this purpose, a method for functionalization of CNTs with ionic liquid having amine group has been developed, and provided to Task III for fabrication.
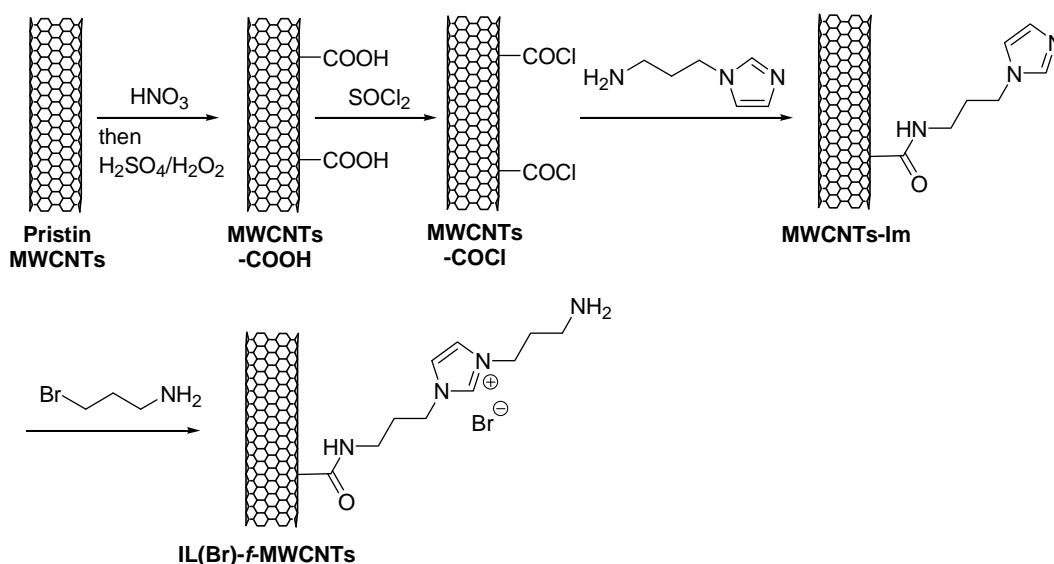
2.3. Accomplishments

2.3.1. Preparation of imidazole-functionalized MWCNTs

We have developed functionalization methods for ionic liquid-carbon nanotubes having amine groups (Fig. 4). The pristine multi-walled carbon nanotubes (MWCNTs) were oxidized by

HNO$_3$ followed by washing with Piranha solution to synthesize carboxylic acid–functionalized MWCNTs (MWCNTs-COOH). The carboxylic acid group was converted to acid chloride (MWCNTs-COCl) by treatment with excess amount of SOCl$_2$ after 24-h reflux. The resulting MWCNTs-COCl reacted with commercially available 3-aminopropyl imidazole at 120°C for 24 h under nitrogen atmosphere. The resulting black solid was filtered through a 0.2-micron poly(tetrafluorethylene) (PTFE) membrane, and successively washed with anhydrous tetrahydrofurane (THF) followed by 1-M aqueous HCl solution, saturated NaHCO$_3$ solution, and water until the pH of the filtrate was 7.0. Elemental analysis indicated 0.76 mmol/g of imidazole moiety was incorporated into the CNT surface. To introduce the amine group, the imidazole-functionalized CNTs were reacted with an excess amount of 3-bromopropylamine hydrobromide in ethanol at 80°C for 24 h. After filtration, the resulting ionic liquid-functionalzed CNTs with amino group (IL(Br)-*f*-MWCNTs) were washed several times with ethanol, H$_2$O, saturated NaHCO$_3$ solution, ethanol, acetone and dried under vacuum at 60°C for 24 h..

Fig. 4. Amine - functionalization of MWCNTs.

1. Objective

The aim of Task III is to develop processing methods for hierarchical carbon fiber (CF) composites and characterize their mechanical and electrical properties.

2. Accomplishments

2.1. Effect of anions in ionic liquids on epoxy curing

Composites were fabricated using three different types of IL functionalized CNTs (f-CNTs): these ionic liquids have Cl^-, PF_6^- and Br^-, respectively. Their curing behavior was studied using differential scanning calorimetry (DSC), Fig. 1. It has been found that Cl- and Br- anions can decrease the degree of cure by oxidizing the curing agent. FTIR and XPS were used to confirm the hypothesis for the ionic liquid containing CL^-, Fig. 2. The hypothesized oxidation mechanism is shown in Fig. 3.

2.2. Processing and characterization of hierarchical CNT-carbon fiber/epoxy composites

2.2.1. Processing

An alumina mold was used to prepare the single-layer and double-layer composites using the hierarchical carbon fiber fabric layers. These carbon fiber fabric layers have CNTs grown upon them in a CVD process as reported in Task I. Depending on whether or not pressure was applied during processing, the fiber volume fraction changed.

All six-layer composites were vacuumed initially to remove air and then hot pressed to obtain higher fiber volume fractions.   SEM images of cross sections are shown in Figs. 5 and 6.

2.2.1. Conductivity

DC conductivity was measured on 3 specimens in the fiber and thickness directions, and TGA was used to measure the fiber volume fraction in composite.   Table 1 summarizes the conductivities of various types of specimens in the fiber direction.   As expected, CNTs improve the conductivity only slightly in the fiber direction.   However, the improvement in the thickness direction can be as high as about two orders of magnitude, Table 2.   Note that the improvement is higher at higher fiber volume contents as a result of shorter distances between CNTs.   The improvements in the 6-layer composites are not as good as those in the 2-layer composites because only two layers in the middle have CNTs.

2.2.2.   Interlaminar fracture toughness

CNTs do not appear to increase the fracture toughness of composite even unless they are aligned in the thickness direction and are close to one another, Figs. 3 and 4.   With increased density, CNTs grow normal to the fiber surface in parallel to one another.   Such alignment appear to be beneficial in improving the interlaminar fracture toughness.
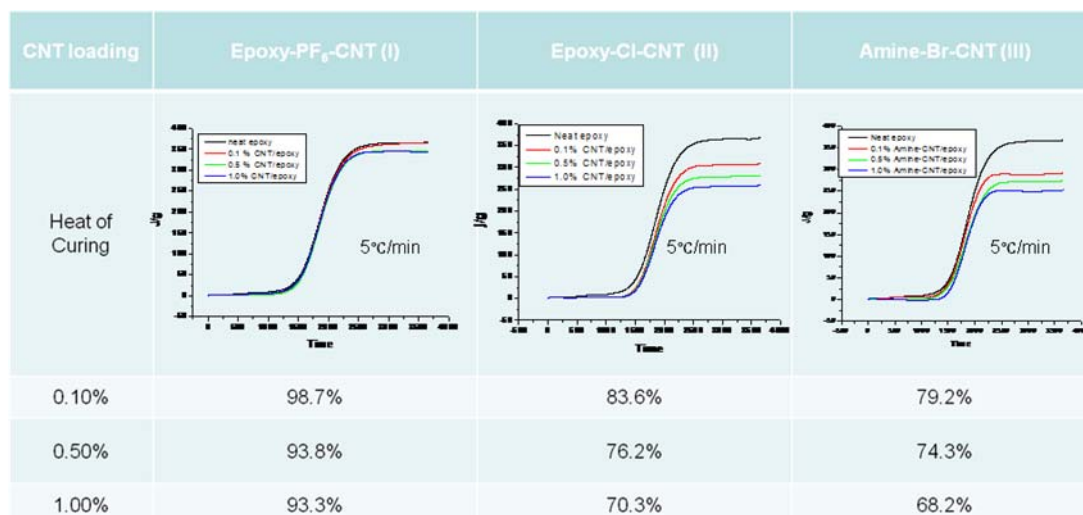

CNT loading	Epoxy-PF$_6$-CNT (I)	Epoxy-Cl-CNT (II)	Amine-Br-CNT (III)
Heat of Curing			
0.10%	98.7%	83.6%	79.2%
0.50%	93.8%	76.2%	74.3%
1.00%	93.3%	70.3%	68.2%

Figure 1.   Degree of cure depending on the type of ionic liquid used.

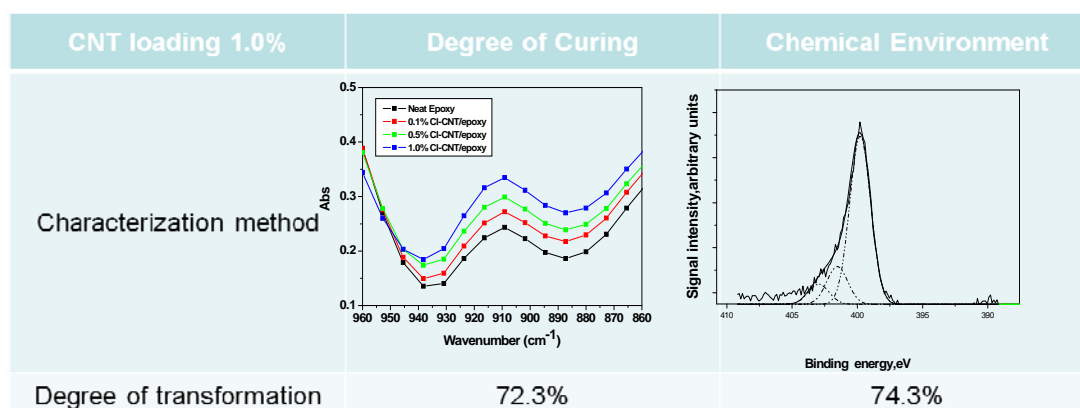| CNT loading 1.0%	Degree of Curing	Chemical Environment
Characterization method		
Degree of transformation	72.3%	74.3%

Figure 2.   Degree of epoxy conversion in 1.0% CNT composite calculated from FTIR and XPS data.
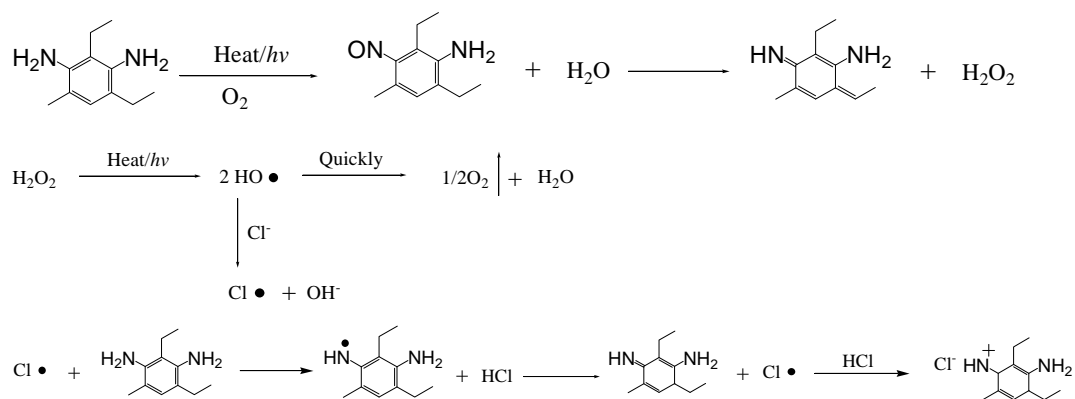
Figure 3.   The possible mechanism of curing agent oxidation induced by CL⁻ anion.

	6-layer CF/Epoxy			6-layer CNT-CF/Epoxy		
	1	2	3	1	2	3
Micrograph						
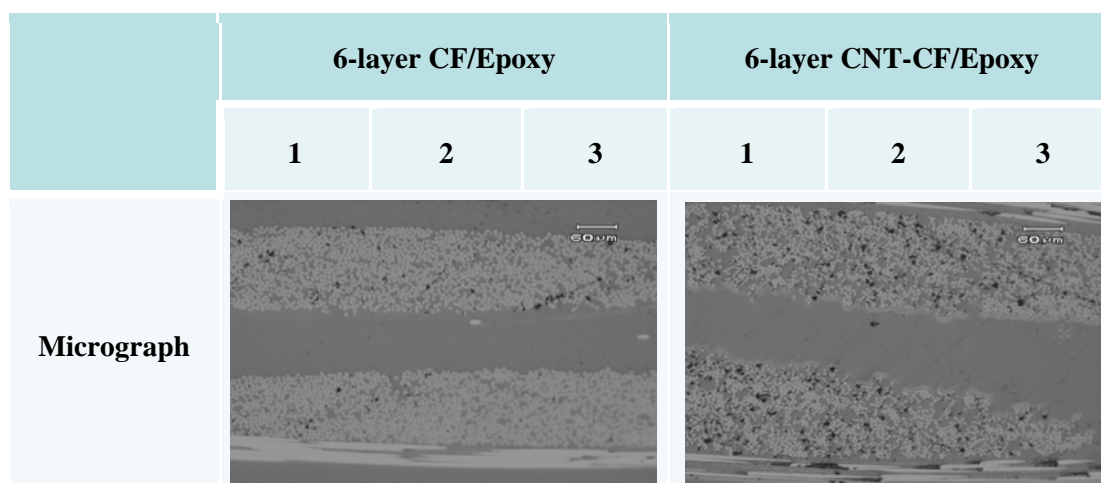
Volume Fraction	19.5	23.2	26.2	16.2	22.3	28.7
Fracture Toughness	376	442	560	194	232	348

Figure 4.   SEM images and fracture toughnesses of composites with low fiber volume fractions
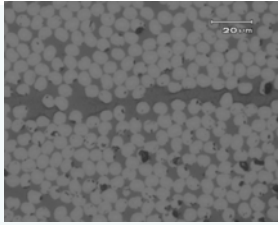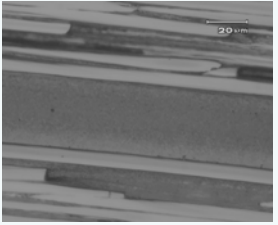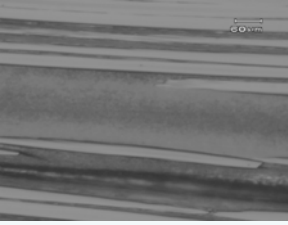
	6-Layer CF/Epoxy	**6-Layer CNT-CF/Epoxy**	
		Low CNT Loading	**High CNT Loading**
Micrograph			
Volume Fraction	60.1	58.8	61.6
Fracture Toughness	241.7 J/m^2	237.2 J/m^2	480.6 J/m^2

Figure 5.   SEM images and fracture toughnesses of composites with high fiber volume fractions.

Table 1. DC conductivities in fiber direction.

			Fiber Volume Fraction	Conductivity (S/cm)	
				Measured	Normalized
Single Layer Fiber		CF	N/A	203.85 (±0.01)	N/A
		Single-Sided CNT-CF	N/A	207.12 (±0.02)	N/A
		Double-Sided CNT-CF	N/A	214.38 (±0.01)	N/A
Single-Layer Composite		CF	23.3 (±0.1)	2.65 (±0.01)	11.37 (±0.01)
		Single-Sided CNT-CF	10.7 (±0.1)	2.26 (±0.02)	21.12 (±0.02)
		Double-Sided CNT-CF	23.1 (±0.1)	5.72 (±0.01)	24.76 (±0.01)
Double-Layer Composite		CF	11.6 (±0.1)	2.56 (±0.02)	22.07 (±0.02)
		Double-Sided CNT-CF	10.8 (±0.1)	3.76 (±0.01)	34.81 (±0.01)

Table 4. DC conductivities of double-layer composites in thickness direction.

Double-Layer Composite		Fiber Volume Fraction %	Conductivity (S/cm)	
			Measured	Normalized
CF	1	17.9	2.2×10^{-4}	1.22×10^{-3}
	2	21.4	9.7×10^{-4}	4.53×10^{-3}
	3	34.5	1.2×10^{-2}	3.48×10^{-2}
	4	60.0	3.6×10^{-2}	6.00×10^{-2}
CNT-CF	1	19.6	3.4×10^{-3}	1.73×10^{-2}
	2	33.6	9.6×10^{-2}	0.28
	3	38.0	0.22	0.58

4	46.2	0.57	1.23
5	58.4	1.72	2.96
6	60.2	2.80	4.65

Table 5. DC conductivities of six-layer composites in thickness direction.

6-Layer Composite		Fiber Volume Fraction (%)	Conductivity (S/cm)	
			Measured	Normalized
CF	1	23.2	4.1×10^{-4}	1.77×10^{-3}
	2	34.5	0.032	9.28×10^{-2}
	3	60.0	0.098	0.16
Low-CNT-CF	1	24.7	4.3×10^{-3}	1.74×10^{-2}
	2	56.3	0.22	0.39
High-CNT-CF	1	58.1	0.32	0.55
	2	60.6	0.48	0.79